

Skin color modeling using the radiative transfer equation solved by the auxiliary function method: inverse problem

Caroline Magnain,* Mady Elias, and Jean-Marc Frigerio

Institut des NanoSciences de Paris, UMR CNRS 7588, Université Pierre et Marie Curie, 140 rue de Lourmel, 75015 Paris, France

*Corresponding author: caroline.magnain@insp.jussieu.fr

Received February 5, 2008; revised April 11, 2008; accepted May 13, 2008;
posted May 14, 2008 (Doc. ID 92406); published June 25, 2008

In a previous article [J. Opt. Soc. Am. A **24**, 2196 (2007)] we have modeled skin color using the radiative transfer equation, solved by the auxiliary function method. Three main parameters have been determined as being predominant in the diversity of skin color: the concentrations of melanosomes and of red blood cells and the oxygen saturation of blood. From the reflectance spectrum measured on real Caucasian skin, these parameters are now evaluated by minimizing the standard deviation on the adjusted wavelength range between the experimental spectrum and simulated spectra gathered in a database. © 2008 Optical Society of America
OCIS codes: 030.5620, 170.3660, 290.4210, 330.1690.

1. INTRODUCTION

Skin color and its variations are important in different fields such as cosmetics, dermatology, and medicine, as well as computer rendering. The diversity of skin colors among people, or according to different locations on the same person, at different times depends mostly on three main characteristic parameters: The concentration of melanosomes, the concentration of red blood cells, and the oxygen saturation of blood. The determination of these three parameters are of great interest. Previous studies to determine one or two of them have used the reflectance and absorbance spectra measured on real skin. For instance, Shimada *et al.* [1] model the light propagation by the modified Beer–Lambert law and use a multiple regression analysis to determine the concentration of melanin and blood. Others use reflectance measurements at selected bands to estimate the melanin index and the erythema index, or the CIELAB coordinates to evaluate the individual typology angle that is related to the skin's pigmentation [2]. Other studies determining the melanin contents in the epidermis needed skin samples to perform a Fontana–Masson stain to distinguish the melanosomes [3]. The results led to absolute values of the volumic concentration. A model based on the real skin structure [4] has previously been developed to study the interaction between the light and all the skin components, such as the melanin, the blood, the keratin, and the collagen. This model takes into account both the absorption and the scattering of each component in every direction. This paper presents an original way to determine these parameters from an experimental reflectance spectrum obtained on real skin with neither sampling nor contact. The method presented in this paper does not need any biopsy of the skin and the melanin concentrations obtained on a computer are also absolute. Moreover, we get two more

pieces of information at the same time: The concentration of blood and the oxygen saturation.

In Section 2, the model used to describe Caucasian skin is recalled. Also recalled are the radiative transfer equation (RTE) which allows one to quantify the interaction of the light through this complex multilayered structure, and its solution through the auxiliary function method (AFM). In Section 3 five parameters of the model are then studied to bring up the main ones responsible for the diversity in human skin color. Finally, in Section 4 the inverse problem is solved. The method consists in the minimization of the standard deviation or of the color change between an experimental spectrum and all the spectra of a database. Both methods are compared and results on real skin reflectance spectra are presented.

2. SKIN COLOR

The skin color is the result of the interaction between light and human skin. The latter is a complex multilayered structure [5] containing various scatterers, either spherical—such as melanosomes and red blood cells—or nonspherical, such as collagen fibers and keratin.

The scatterers are in low concentration, which implies that when an incoherent light goes through it, it stays incoherent. That is the reason why the RTE can be used to model the interaction between light and the skin, first developed by Chandrasekhar [6] for the neutron scattering. To implement an exact solution the AFM is used [7].

A. Skin Model

We have previously defined and validated a model based on the real structure of Caucasian skin (Fig. 1) [4] inspired by Nielsen *et al.* [8]. First there is the upper main layer, the epidermis, made of five sublayers containing

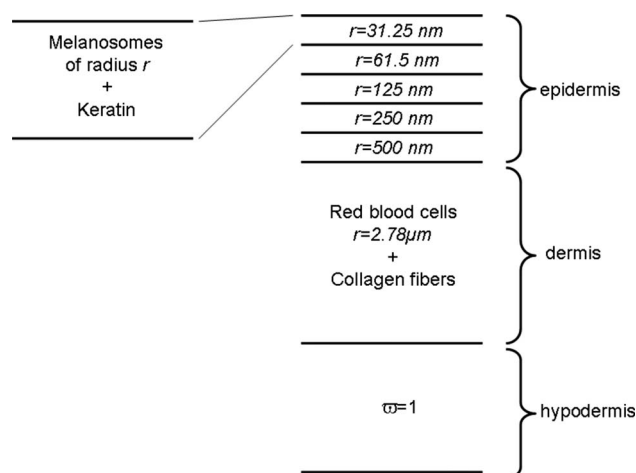


Fig. 1. Skin structure.

the melanosomes with a constant volumic concentration C , which varies between 1% and 7.5% for Caucasian skin [9,10]. These scatterers are produced in the lower sub-layer, the *stratum basale*. As the cells move up in the epidermis, they shorten [11]. We consider them as spherical with a radius lying between 500 and 31.25 nm [8]. Keratin is also found in the epidermis. The thickness of the whole epidermis z_e is of several tens of micrometers.

Then there is the intermediate layer, the dermis, which contains the red blood cells. They are biconcave disks but in order to use Mie theory we consider them as spherical with a radius of $2.78\text{ }\mu\text{m}$ [12], which allows them to have the same volume. It has been proved to be appropriate when evaluating the scattering cross sections [13]. Their volumic concentration is noted as CS and lies mostly between 1% and 5% [14]. Blood is made, among other substances, of deoxyhemoglobin (Hb) and oxyhemoglobin (HbO_2) with different properties as their complex refractive index [12,15]. Let S be the oxygen saturation, meaning the percentage of oxyhemoglobin. This percentage depends on the location, in veins or arteries, from 47% to almost 100% [9]. Collagen fibers are also found in the dermis. The thickness of the dermis z_d can reach several millimeters.

Finally, there is the hypodermis, which contains mainly lipids and blood. However we consider that the lipids are here predominant and therefore that the hypodermis only scatters the light. The thickness of the hypodermis goes from none to several centimeters.

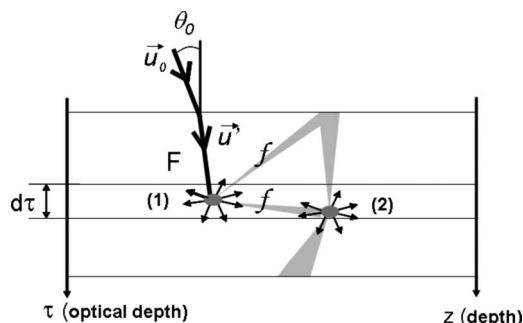


Fig. 2. Scattering in a complex medium.

B. Radiative Transfer Equation and the Auxiliary Function Method

The RTE expresses the diffuse flux balance through an elementary scattering and homogeneous slab with an optical thickness $d\tau$ for a given wavelength λ and a given direction symbolized by the unit vector \mathbf{u} .

The incident beam is here considered as collimated in the direction \mathbf{u}_0 , which can stay collimated (flux F), or become diffuse (flux f) as shown in Fig. 2. It writes

$$\mu \frac{df(\mathbf{u}, z)}{dz} = -(k+s)f(\mathbf{u}, \tau) + \frac{s}{4\pi} F(\mathbf{u}', z) p(\mathbf{u}, \mathbf{u}') + \frac{s}{4\pi} \int_0^{4\pi} f(\mathbf{u}_1, z) p(\mathbf{u}, \mathbf{u}_1) d\Omega_1, \quad (1)$$

where k and s are, respectively, the absorption and the scattering coefficients of the scatterers (in m^{-1}) and z is the thickness. It writes with the reduced quantities, the albedo $\omega = s/(s+k)$ and the optical depth $\tau = (k+s)z$,

$$\frac{df(\mathbf{u}, \tau)}{d\tau} = -\frac{f(\mathbf{u}, \tau)}{\mu} + \frac{\omega}{4\pi} \frac{\mu}{|\mu|} \frac{F(\mathbf{u}', \tau)}{|\mu'|} p(\mathbf{u}, \mathbf{u}') + \frac{\omega}{4\pi} \frac{\mu}{|\mu|} \int_0^{4\pi} \frac{f(\mathbf{u}_1, \tau)}{|\mu_1|} p(\mathbf{u}, \mathbf{u}_1) d\Omega_1, \quad (2)$$

with $\mu = \cos \theta$.

The first term on the right-hand side corresponds to the light decrease due to the scattering and the absorption of the scatterers. The second term expresses the simple scattering of the collimated light [labeled (1) in Fig. 2]. The third term expresses the multiple scattering [labeled (2) in Fig. 2]. The medium is characterized by the albedo ω and the optical thickness τ . The phase function $p(\mathbf{u}, \mathbf{u}_1)$ also characterizes the scatterers by the proportion of light coming with the direction \mathbf{u}_1 and scattered in the direction \mathbf{u} .

The AFM, already developed in our group [7,16], is used to solve the RTE. The multiple scattering term is replaced by an auxiliary function [third term on the right-hand side of Eq. (2)]. An exact system of integral Fredholm equations relative to the auxiliary function is then obtained instead of integrodifferential ones where the different directions are uncoupled. No assumptions are needed for further calculations. And contrary to other methods (Nflux [17], discrete ordinate method [18], etc.), there is no need for an angular discretization. The auxiliary function is calculated, which leads to the diffuse flux f that determines the reflectance factor for each wavelength and therefore the diffuse reflectance spectrum. The detailed calculations can be found in previous papers [4,16].

We applied this equation to our previously discussed skin model. The incident light is set at normal incidence. The diffuse flux is integrated over the upper half of the space. The simulated spectra obtained by this modeling have been validated with experimental spectra measured on different persons. A Cary spectrometer (Varian), coupled with an integration sphere including the specular light, is used to measure those spectra in the same configuration, $0^\circ/\text{diffuse}$, as the modeling.

Five parameters can be adjusted: The concentrations of melanosomes C and red blood cells CS , the oxygen saturation S , and the thicknesses of the epidermis z_e and of the dermis z_d . The variables ϖ , τ , and $p(\mathbf{u}, \mathbf{u}_1)$ are either taken from the literature [10,19] or calculated using Mie theory [20].

3. INFLUENCE OF THE PARAMETERS

The reflectance spectra measured on real skin are different from one individual to another as well as for two different locations on the same person. The color of the skin also depends on the conditions of the experiment: The room hydrometry and temperature for instance. All these color differences can be explained by different values of only five characteristic parameters: The thicknesses of the dermis z_d and of the epidermis z_e , the oxygen saturation of the blood S , and the concentrations of the red blood cells CS and the melanosomes C .

The influence of each parameter on the reflectance spectra is studied within their physiological boundaries [9,10,14] in order to identify the ones that are the most responsible for the diversity of Caucasian skin colors. Each spectrum is associated with a color in the CIELAB space defined in 1976 [21] that can be described by three coordinates: L^* , the lightness; a^* , the green–red coordinate; and b^* , the blue–yellow coordinate. The D 65 illuminant and the 2° standard observer have been used for the calculations. The color change ΔE between two extreme spectra numbered 1 and 2 is then defined by

$$\Delta E = \sqrt{(L_1^* - L_2^*)^2 + (a_1^* - a_2^*)^2 + (b_1^* - b_2^*)^2}. \quad (3)$$

One is said to distinguish two colors if the color change between them is more than 2.

Table 1 summarizes the color change ΔE between two spectra obtained with the extreme values of one parameter (bold) and the other ones fixed. First, the influence of the dermal thickness z_d is studied for values from 1 to 2 mm. The difference between the corresponding simulated spectra cannot explain how the skin color can be so different from one to another. Actually, the corresponding color change ΔE in the CIELAB space is only of 1.34, which is too small to be relevant.

Second, the thickness of the epidermis z_e varies from 40 to 70 μm . In the same manner, the separation between the extreme spectra is not large enough to explain the difference in the human complexions. The corresponding

Table 1. Influence of Each Parameter on the Color Change ΔE Calculated between the Two Extreme Values^a

z_d (mm)	z_e (μm)	S (%)	CS (%)	C (%)	ΔE
1–2	50	70	2	1.5	1.34
2	40–70	70	2	1.5	1.66
2	50	50–90	2	1.5	3.09
2	50	70	1–5	1.5	10.71
2	50	70	2	1.5–7.5	12.86

^aBold indicates one parameter; lightface indicates fixed parameters.

color change ΔE for this extreme variation of the thickness is only equal to 1.66, which is once more too small.

Then, we study the difference in the spectra due to the variation of the oxygen saturation of the blood (S). The shape of the spectra between 430 and 530 nm changes with the variation of the oxygen saturation. Moreover, a peak appears at 560 nm as S increases [4]. The main variation is the increase of the reflectance factor with S for larger wavelengths, corresponding to a plateau. This parameter thus explains the change of shape of the real skin spectra. Actually the color change ΔE is equal to 3.09 between the spectra with the extreme values $S=50\%$ and 90% . At the same time, a^* and b^* increase, meaning that the skin is redder and less blue, consistent with the increase of the oxygen saturation.

The influence of the volumic concentration of red blood cells (CS) is then studied. As CS increases, the reflectance spectrum is translated downwards [4]. This parameter covers a wide range of reflectance spectra and is important for the modeling of the skin color. The color change between the spectra with $CS=1\%$ and $CS=5\%$ is 10.71. As CS increases, the lightness L^* decreases and a^* increases, meaning that the skin becomes darker and redder.

Finally, the influence of the volumic concentration of melanosomes is the most important and the different spectra are recalled on Fig. 3. That is what makes the difference between Caucasian and negroid skin. The larger the melanosomes concentration, the darker the skin. The color change ΔE is equal to 12.86 between the spectra of concentration C varying between 1.5% and 7.5%. It is the lightness L^* that mainly decreases as C increases.

The three main parameters that can explain the difference in color complexion among people are, therefore, the volumic concentration of melanosomes (C), the volumic concentration of red blood cells (CS), and the oxygen saturation (S). Afterwards we will try to find only these three parameters from an experimental skin spectrum and we will fix the two others to their mean values: $z_e=50 \mu\text{m}$ and $z_d=2000 \mu\text{m}$.

4. INVERSE PROBLEM

To solve the inverse problem, i.e., to determine the values of the three previous characteristic parameters corresponding to an experimental reflectance spectrum of real Caucasian skin, the main process will be to minimize a function depending on the difference between the experimental spectrum and numerous spectra calculated and gathered in a database. This function can come from a geometric difference between the spectra and the standard deviation ϵ is then required. It can also be directly tied to the trichromatic coordinates and the color change ΔE is then required. It must be noticed that the wavelength range is adjustable in the first case, but is strictly dictated by the visible range in the second case.

A. Solving Method

1. Database

To build a database of reference spectra and to later compare an experimental skin spectrum with all of them, ref-

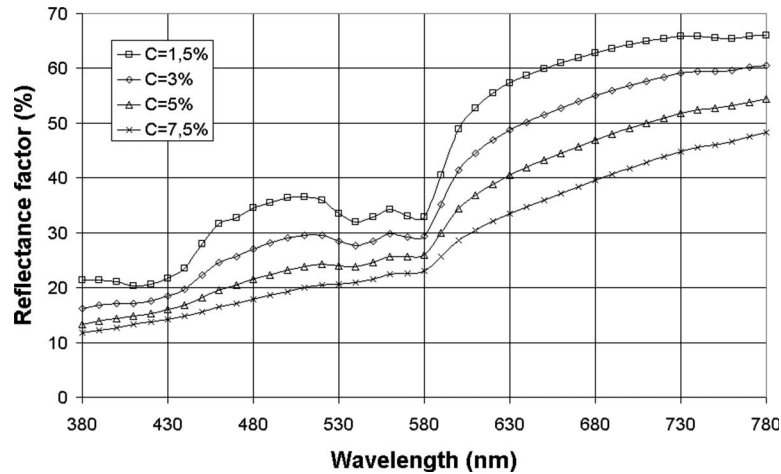


Fig. 3. Influence of the volumic concentration of melanosomes C on the modeled reflectance spectrum of Caucasian skin.

erence spectra are first generated for all the possible combinations obtained for seven concentrations of melanosomes C , seven concentrations of red blood cells CS ; and three oxygen saturations of the blood S , which cover the physiological ranges.

- C : [0.01% 1.5% 3% 4.5% 6% 7.5% 9%]
- CS : [0.5% 2% 2.75% 3.5% 4.25% 5% 9%]
- S : [50% 70% 90%]

The ranges of variation of C and CS are extended to two extreme values, 0.01%–9% and 0.5%–9%, respectively, in order to avoid any further nonrelevant extrapolation outside the physiological ranges. Only three oxygen saturations S are used because it has been previously shown that this parameter does not influence the skin color a lot.

The calculations of the previous simulated reference spectra lead to reflectance factors for 41 wavelengths depending on C , CS , and S . To increase the accuracy of the further adjustment with an unknown spectrum, a quadratic interpolation is implemented around the nearest closest reference (NCR). It consists in evaluating a reflectance factor for each wavelength defined on the rectangular three-dimensional grid C , CS , and S , by the quadratic polynomial

$$R(\lambda, C, CS, S) = a + \sum_{x=C, CS, S} (b_x x + c_x x^2) + \frac{1}{2} \sum_{x=C, CS, S} \sum_{y=C, CS, S \neq x} d_{x,y} x \cdot y, \quad (4)$$

where $d_{x,y} = d_{y,x}$.

The ten adjustable constants a , b_x , c_x , and $d_{x,y}$ are determined by the values of the ten nearest reference points surrounding NCR.

2. Validation

Let $R_{\text{unknown}}(\lambda_i)$ and $R_{\text{ref}}(\lambda_i)$ be the reflectance factors of the unknown spectrum and of one of the reference spectra. Let ϵ be the standard deviation between them defined by

$$\epsilon = \sqrt{\frac{\sum_{i=1}^{i_{\max}=41} (R_{\text{unknown}}(\lambda_i) - R_{\text{ref}}(\lambda_i))^2}{i_{\max} - 1}}, \quad (5)$$

and ΔE be [Eq. (3)] the color change also calculated between the same spectra.

The process uses a quasi-Newton method to find the minimum of the function ϵ or ΔE depending on the three variables C , CS , and S . It leads to three values of the three parameters corresponding to the best match.

In a preliminary step this inverse solving has been tested on 21 spectra that we have simulated with known parameters, different from the ones used for building the database. Table 2 shows the relative error (in percentages) for each parameter, using either the minimization of the standard deviation ϵ or the minimization of the color change ΔE .

The parameters obtained by the inverse solving process are in quite good agreement with those used to obtain the simulated spectra. The method can now be applied to measured reflectance spectra of real skin for which the previous parameters are unknown. It can be noticed that the minimization of ϵ leads to better results for C and S . Moreover, in this case, the wavelength range can be adapted to a more significant one.

To improve the method, the range of wavelengths used to calculate the standard deviation is then discussed and adjusted. The results obtained by the minimization of the standard deviation calculated in the adequate range and of the color change calculated in the whole visible range are then compared.

Table 2. Relative Error in Percentages on the Determination of the Parameters C , CS , and S for Both Minimizations of ϵ or ΔE

Parameters	Method ϵ	Method ΔE
C	1.4%	2.8%
CS	4.9%	3.4%
S	1.9%	3.74%

Table 3. Parameters Obtained by Minimizing the Standard Deviation Calculated over the Ranges 380–780 nm and 380–600 nm and the Values of ϵ for a Real Skin Spectrum

Parameters	380–780 nm	380–600 nm
ϵ	3.44	0.51
C	1.5	1.13
CS	6.85	6.21
S	49.15	63.65

B. Wavelength Range for Standard Deviation Calculation

In a previous paper [4], we have shown that our modeling process can lead to spectra with a very different reflectance factor for large wavelengths (red color), mostly higher than those of the measured spectra. We used the reduced scattering coefficient $s' = s(1-g)$ for the red blood cells where g is the asymmetry factor. As shown in [13], this factor is overestimated with Mie theory because of their real shape. This could explain the difference between the real spectrum and the simulated ones since the blood cells are responsible for the shape of the spectra at this range and since the absorption of melanosomes is low. Nevertheless this difference does not clearly emerge in the color change, which uses all of the visible range, because the human eye and then the standard observer is less sensitive to the large wavelengths. In the case of the minimization of the standard deviation, it is possible to limit and adjust the wavelength range. We here compare the results using this method on the whole visible range and on a smaller wavelength range from 380 to 600 nm on a real skin spectrum with unknown parameters. The val-

ues of the obtained parameters C , CS , and S are slightly different but the standard deviation is always smaller for the restrained domain, as summarized in Table 3.

Figure 4 shows the spectrum of this Caucasian skin (solid curve) and the modeled spectra corresponding to the best match and obtained first by taking into account the whole visible range (squares) and second by taking into account the narrow range 380–600 nm (triangles). Obviously, better results for the spectra and the standard deviation are obtained by considering the narrow range 380–600 nm. Moreover, the parameters obtained by using the whole visible range can sometimes leave the biological boundaries.

C. Minimization of ϵ or ΔE

One can think that the effect of the previous reduced wavelength range used to calculate the standard deviation is equivalent to the function of the standard observer used to calculate the color change, which reduces the perception of the large wavelengths. So, both methods are now compared for solving the inverse problem: The minimization of the color change or the standard deviation over the range 380–600 nm. Table 4 shows the parameters obtained by using the software for the 11 different real skin reflectance spectra.

The calculated values of the parameters are quite similar and biologically relevant for the concentration of melanosomes C and for the concentration of red blood cells CS . However for the oxygen saturation S , the minimization of the color change leads to some values outside the biological range: S can be greater than 100% or smaller than 47% [9] as shown in Fig. 5 for the 11 previous cases.

Thus, for the minimization of the color change, 8 out of 11 values of S leave the biological limits, whereas all but

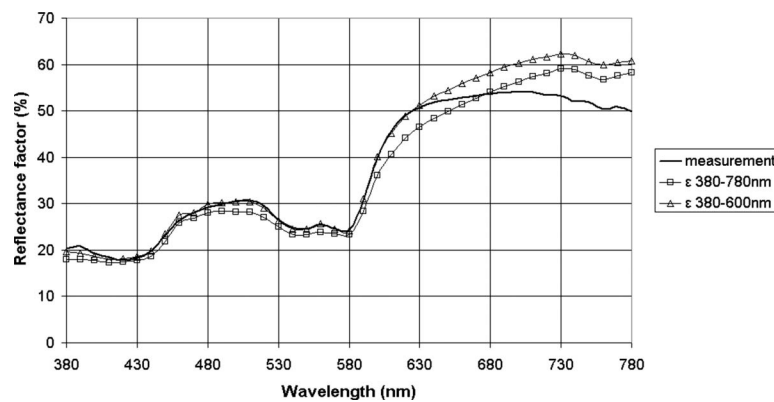


Fig. 4. Results of the inverse problem for a measurement (solid curve), the minimization of the standard deviation ϵ is realized on 380–780 nm (squares) and 380–600 (triangles).

Table 4. Determination of the Parameters of the 11 Measured Reflectance Spectra for Both Methods

Method	Spectrum	1	2	3	4	5	6	7	8	9	10	11
ΔE (380–780 nm)	C	1.7	3.0	2.2	9.4	4.0	1.8	1.4	2.2	1.8	2.5	1.4
	CS	1.1	1.3	5.4	0.7	4.5	1.4	1.6	1.1	0.7	1.0	5.6
	S	81.4	131.1	64.4	173.0	108.9	112.0	10.2	25.3	29.2	30.6	60.5
ϵ (380–600 nm)	C	1.7	2.1	1.6	8.3	2.6	1.4	1.3	2.1	1.8	2.6	1.1
	CS	1.1	2.2	6.4	2.3	6.7	1.7	1.7	1.3	0.8	1.0	6.2
	S	67.5	85.9	59.4	103.5	81.1	88.0	62.0	35.2	46.9	37.3	63.6

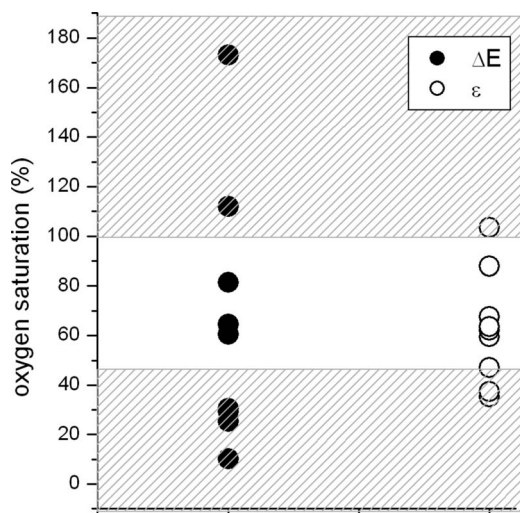


Fig. 5. Values of the oxygen saturation S obtained for 11 reflectance spectra for both methods, the minimization of the color change ΔE (solid circles) and the standard deviation ϵ on 380–600 nm (open circles). Unrealistic values for S have been shaded.

three are consistent with the biological range using the minimization of the standard deviation calculated over the domain 380–600 nm. The ones outside the range are less unrealistic than the ones obtained with the minimization of the color change.

The best method to find the values of the main three parameters is then the minimization of the standard deviation ϵ over the range 380–600 nm. It can be noticed that the biological ranges are the only possible validation and that there is no tool to choose between two close values of C , CS , and S inside these ranges.

Figure 6 shows four measured spectra (solid curves) and the best match simulated spectra (symbols) corresponding to the first four cases of Table 4. The calculated reflectances are also in good agreement with the ones of real skin, although they branch off for the larger wavelengths.

The solving of the inverse problem presented here is still limited to pale Caucasian skin. Actually, for the lower spectrum No. 4 the oxygen saturation S exceeds 100%, which is inconsistent with the biological boundaries. The small value of the reflectance factor means that the Cau-

casian skin is really tanned, which is also shown by an important concentration of melanosomes C of 8.3%. It is then harder to determine the parameters when the concentration of melanosomes increases because the spectrum is then smoothed. Moreover it also shows the limitation of the used model (Fig. 1), that has been validated for Caucasian skin but cannot be applied as it is for darker skin such as highly tanned Caucasians, Negroids, or Mongoloids.

5. CONCLUSION

To study Caucasian skin color a complex multilayered model has been previously developed, based on the real skin structure. The radiative transfer equation describes the interaction between light and matter and the auxiliary function method is used to solve it. The color of Caucasian skin depends on three main characteristic parameters, which are the concentration of the melanosomes, the concentration of the red blood cells, and the oxygen saturation. The model has been validated for different real skin spectra measured with a Cary spectrometer. This paper deals with the inverse problem, the determination of the three main parameters from an experimental reflectance spectrum obtained on real skin. The software developed for this purpose uses the minimization of standard deviation calculated over the range 380–600 nm between the experimental spectrum and a database of simulated spectra. It has been validated on reflectance spectra simulated with known parameters different from the database ones. This software has then been used to determine the three parameters of 11 experimental spectra of Caucasian persons. The obtained values of the characteristic parameters belong to the biological ranges and are satisfactory for Caucasian skin. Solving the problem can also be very helpful for the biomedical field to statistically study the evolution of C , CS , and S according to the location of the skin or of the origin of the person.

The evolution of skin color as well as the evolution of each of the three main characteristic parameters could now be easily studied according to different factors such as the UV exposure of the skin *in vivo*, without any sampling (biopsies). In particular, the evolution of the melanin content could be studied. This method could also be used for early detection of skin diseases.

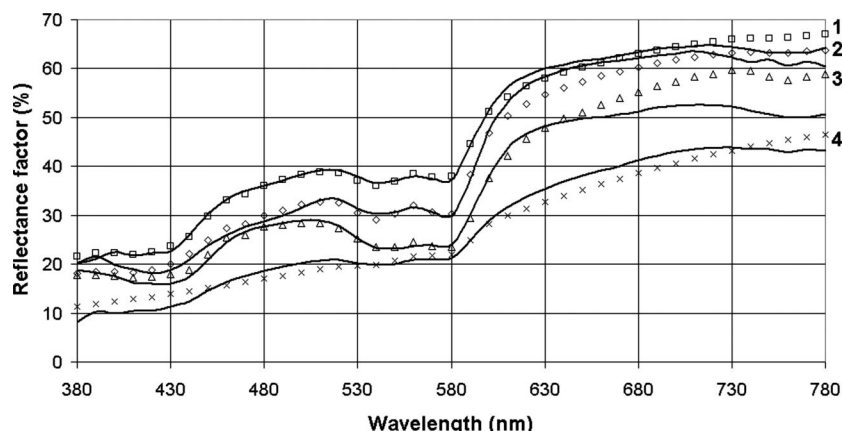


Fig. 6. Four real skin reflectance spectra (solid curves) and their simulated spectra (symbols) calculated with our method.

The database and the inverse problem solving are going to be extended with configurations other than the 0°/diffuse. A portable goniospectrometer in a backscattering configuration has been developed in our laboratory and will be used to measure skin reflectance spectra.

REFERENCES

1. M. Shimada, Y. Yamada, M. Itoh, and T. Yatagai, "Melanin and blood concentration in human skin studied by multiple regression analysis: Experiments," *Phys. Med. Biol.* **46**, 2385–2395 (2001).
2. G. N. Stamatas, B. Z. Zmudzka, N. Kollias, and J. Z. Beer, "Non-invasive measurements of skin pigmentation *in situ*," *Pigment Cell Res.* **17**, 618–626 (2004).
3. T. Tadokoro, Y. Yamaguchi, J. Batzer, S. G. Coelho, B. Z. Zmudzka, S. A. Miller, R. Wolber, J. Z. Beer, and V. J. Hearing, "Mechanisms of skin tanning in different racial/ethnic groups in response to ultraviolet radiation," *J. Invest. Dermatol.* **124**, 1326–1332 (2005).
4. C. Magnain, M. Elias, and J. M. Frigerio, "Skin color modeling using the radiative transfer equation solved by the auxiliary function method," *J. Opt. Soc. Am. A* **24**, 2196–2205 (2007).
5. L. A. Goldsmith, *Physiology, Biochemistry, and Molecular Biology of the Skin* (Oxford U. Press, 1998).
6. S. Chandrasekhar, *Radiative Transfer* (Dover, 1960).
7. M. Elias and G. Elias, "New and fast calculation for incoherent multiple scattering," *J. Opt. Soc. Am. A* **19**, 894–901 (2002).
8. K. P. Nielsen, L. Zhao, P. Juzenas, J. J. Stamnes, K. Stamnes, and J. Moan, "Reflectance spectra of pigmented and nonpigmented skin in the UV spectral region," *Photochem. Photobiol.* **80**, 450–455 (2004).
9. E. Angelopoulou, "The reflectance spectrum of human skin," Tech. Rep. No. MS-CIS-99-29, Department of Computer and Information Science, University of Pennsylvania (1999), pp. 1–14.
10. S. L. Jacques, <http://omlc.ogi.edu/news/jan98/skinoptics.html> (1998).
11. R. R. Anderson and J. A. Parrish, "Optical properties of human skin," in *The Science of Photomedicine* (Plenum, 1982), pp. 147–194.
12. D. J. Faber, M. C. G. Aalders, E. G. Mik, B. A. Hooper, M. J. C. van Gemert, and T. G. van Leeuwen, "Oxygen saturation-dependent absorption and scattering of blood," *Phys. Rev. Lett.* **93**, 028102, 1–4 (2004).
13. J. M. Steinke and A. P. Sheperd, "Comparison of Mie theory and the light scattering of red blood cells," *Appl. Opt.* **27**, 4027–4033 (1988).
14. G. Poirier, "Human skin modelling and rendering," Master's thesis (University of Waterloo, 2004).
15. S. L. Jacques, <http://omlc.ogi.edu/spectra/hemoglobin/index.html> (1999).
16. M. Elias and G. Elias, "Radiative transfer in inhomogeneous stratified scattering media with use of the auxiliary function method," *J. Opt. Soc. Am. A* **21**, 580–589 (2004).
17. P. S. Mudgett and L. W. Richards, "Multiple scattering calculations for technology," *Appl. Opt.* **10**, 1485–1502 (1971).
18. K. Stamnes, S. Chee Tsay, W. Wiscombe, and K. Jayaweera, "Numerically stable algorithm for discrete-ordinate-method radiative transfer in multiple scattering and emitting layer media," *Appl. Opt.* **27**, 2502–2510 (1988).
19. M. J. C. van Gemert, S. L. Jacques, H. J. C. M. Sterenborg, and W. M. Star, "Skin optics," *IEEE Trans. Biomed. Eng.* **36**, 1146–1154 (1989).
20. C. F. Bohren and D. R. Hoffman, *Absorption and Scattering of Light by Small Particles* (Wiley-VCH, 1983).
21. G. Wyszecki and W. S. Stiles, *Color Science: Concepts and Methods, Quantitative Data and Formulae*, 2nd ed. (Wiley Interscience, 1982).